NRC Publications Archive
Archives des publications du CNRC

Direct space methods for powder X-ray diffraction for guest-host materials : applications to cage occupancies and guest distributions in clathrate hydrates

Takeya, Satoshi; Udachin, Konstantin A.; Moudrakovski, Igor L.; Susilo, Robin; Ripmeester, John A.

National Research Council Canada   Conseil national de recherches Canada

Canada

Direct Space Methods for Powder X-ray Diffraction for Guest−Host Materials: Applications to Cage Occupancies and Guest Distributions in Clathrate Hydrates

Satoshi Takeya,[†] Konstantin A. Udachin, Igor L. Moudrakovski, Robin Susilo, and John A. Ripmeester*

Steacie Institute for Molecular Sciences, National Research Council Canada, 100 Sussex Drive, Ottawa, Ontario, K1A OR6, Canada

Received July 2, 2009; E-mail: john.ripmeester@nrc-cnrc.gc.ca

Abstract: Structural determination of crystalline powders, especially those of complex materials, is not a trivial task. For non-stoichiometric guest−host materials, the difficulty lies in how to determine dynamical disorder and partial cage occupancies of the guest molecules without other supporting information or constraints. Here, we show how direct space methods combined with Rietveld analysis can be applied to a class of host−guest materials, in this case the clathrate hydrates. We report crystal structures in the three important hydrate crystal classes, sI, sII, and sH, for the guests CO_2, C_2H_6, C_3H_8, and methylcyclohexane + CH_4. The results obtained for powder samples are found to be in good agreement with the experimental data from single crystal X-ray diffraction and ^{13}C solid-state NMR spectroscopy. This method is also used to determine the guest disorder and cage occupancies of neohexane and *tert*-butyl methyl ether binary hydrates with CH_4 in the structure H clathrate hydrates. The results are found to be in good agreement with the results from the ^{13}C solid-state NMR and molecular dynamics simulations. It is demonstrated that the ab initio crystal structure determination methodology reported here is able to determine absolute cage occupancies and the dynamical disorder of guest molecules in clathrate hydrates from powdered crystalline samples.

Introduction

It is of paramount importance to develop the best models of guest−host interactions in supramolecular materials so as to improve our understanding of the multiple weak interactions that often determine their structures and useful properties.[1] Today, materials of ever increasing complexity are being synthesized, including metal oxide frameworks (MOFs),[2−4] enzyme mimics,[5] and other bioactive materials,[6−8] as well as a variety of guest−host materials.[9,10] Clathrate hydrates, also known as gas hydrates, are hydrate guest−host compounds and are crystalline materials consisting of water molecules that are hydrogen-bonded to form host cages that include guest molecules inside the cages.[1] Natural gas hydrates, now seen as a possible global source of relatively clean energy, require characterization of their stoichiometry in order to give good estimates of their resource potential.[11] Also, the capability of gas hydrates to store large amounts of gas with considerable selectivity based on guest gas properties has opened up possibilities for potential industrial applications such as gas storage and/or gas separation, including greenhouse gas capture.[12−14] Although the water clathrates are perhaps the best understood guest−host materials regarding structural, thermodynamic, and other physical properties, there are still problems in characterizing such materials. For instance, guest−host interactions play a crucial role as gas hydrates are thermodynamically stable only when a minimum number of cages are occupied by the guest molecules, depending on their nature. In practice it has been found that the largest cage in the hydrate structures needs to be completely filled or nearly so. The actual stoichiometry then depends on the details of conditions during synthesis, both in the laboratory and in nature, and the type of

[†] Permanent address: National Institute of Advanced Industrial Science and Technology (AIST), Central 5, Higashi 1-1-1, Tsukuba 305-8565, Japan

(1) *Comprehensive Supramolecular Chemistry*; Atwood, L. L., Davies, D., MacNicol, D. D., Vogtle, F., Eds.; Pergamon/Elsevier: Oxford, 1996.

(2) Yaghi, O. M.; O'Keeffe, M.; Ockwig, N. W.; Chae, H. K.; Eddaoudi, M.; Kim, J. *Nature* **2003**, *423*, 705−714.

(3) Matsuda, R.; Kitaura, R.; Kitagawa, S.; Kubota, Y.; Belosludov, R. V.; Kobayashi, T. C.; Sakamoto, H.; Chiba, T.; Takata, M.; Kawazoe, Y.; Mita, Y. *Nature* **2005**, *436*, 238−241.

(4) Britt, D.; Tranchemontagne, D.; Yaghi, O. M. *Proc. Natl. Acad. Sci. U.S.A.* **2008**, *105*, 11623−11627.

(5) Kirby, A. *Angew. Chem., Int. Ed.* **1996**, *35*, 707−724.

(6) Hapiot, F.; Tilloy, S.; Monflier, E. *Chem. Rev.* **2006**, *106*, 767−781.

(7) Lagona, J.; Mukhopadhyay, P.; Chakrabarti, S.; Isaacs, L. *Angew. Chem., Int. Ed.* **2005**, *44*, 4844−4870.

(8) Bardelang, D.; Banaszak, K.; Karoui, H.; Rockenbauer, A.; Waite, M.; Udachin, K.; Ripmeester, J. A.; Ratcliffe, C. I.; Ouari, O.; Tordo, P. *J. Am. Chem. Soc.* **2009**, *131*, 5402−5404.

(9) Müller, A.; Reuter, H.; Dillinger, S. *Angew. Chem., Int. Ed.* **1995**, *34*, 2328−2361.

(10) Kitagawa, S.; Kitaura, R.; Noro, S. *Angew. Chem., Int. Ed.* **2004**, *43*, 2334−2375.

(11) *Natural Gas Hydrate in Oceanic and Permafrost Environments*, Max, M. D., Ed.; Kluwer Academic Publishers: The Netherlands, 2003.

(12) Englezos, P.; Lee, J. D. *Korean J. Chem. Eng.* **2005**, *22*, 671−681.

(13) Sloan, E. D. *Nature* **2003**, *426*, 353−359.

(14) Park, Y.; Kim, D. Y.; Lee, J. W.; Huh, D. G.; Park, K. P.; Lee, J.; Lee, H. *Proc. Nat. Acad. Sci. U.S.A.* **2006**, *106*, 12690−12694.
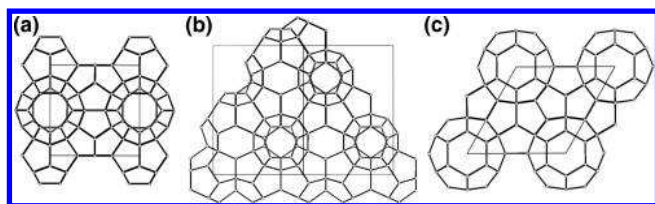
Figure 1. Ball-and-stick representation of gas hydrates. The solid line in each figure denotes the unit cell of the gas hydrate. (a) Structure I, (b) structure II, and (c) structure H.

guest molecule. It is actually a lengthy time-consuming process to prepare hydrates with true equilibrium compositions.

The three main structural families of gas hydrate are well-known and depend mainly on the van der Waals diameter of the guest molecules and the relative number of large and small cages in the different structures: structure I with space group *Pm3n*, structure II with space group *Fd3m*, and structure H with space group *P6/mmm* (see Figure 1).[15−18] We note that there are few nondestructive characterization methods of gas hydrates that give both structural information and compositions. Single crystal diffraction is one of these, although it is difficult to obtain and handle single crystals of gas hydrates, and there are limits on how many guests can be distinguished. NMR spectroscopy is quite diagnostic for structure and composition, although this method tends to give relative rather than absolute cage occupancies. Raman spectroscopy is of use for some specific guests, although there are problems in knowing the scattering cross sections for enclathrated guests. Powder diffraction has been used, both X-ray and neutron, but as we shall show in this work, often unjustified assumptions have to be made because of the low data-to-parameter ratios and the coupling of parameters that lead to significant errors and uncertainties.

The three common hydrate crystal structures and other gas hydrates structures have been confirmed by the single crystal X-ray diffraction technique.[19−24] However, modeling of the guest molecules in the hydrate cages is not trivial, even though single crystals of sufficient size and good quality are available.[25] The exact positions and number of the disordered guest molecules in structural studies continues to be a serious challenge because it is necessary to solve the electron map difference inside the cages by careful analysis. Although single crystal X-ray diffraction is still the best tool for determining crystal structures, it is not always applicable, for instance, for solid materials for which it is difficult to grow single crystals, including gas hydrates. As mentioned before, traditional powder diffraction methods suffer from greater uncertainties largely because of the unfavorable data-to-parameter ratios. The

complexity of the problem generally depends on the number of atoms to be located in the asymmetric unit. Consequently, many crystal structures of gas hydrates have been solved by assuming the center of the disordered guest molecules to be at the center of the cages[26−36] and by using the Rietveld refinement technique.[37] Recently, significant advances have been made in other approaches to solving structures from powder diffraction data. For instance, the structures of various materials have been obtained through computer modeling[38,39] even for the characterization of complex materials.[40] Therefore, structural characterization techniques using the powder method is still powerful strategy for improving our understanding of the structure and dynamics of many important solid materials. Direct-space techniques using powder diffraction overcome the intrinsic problems encountered in the structure-solution stage of the structural determination process with powder diffraction.[41] Trial structures are generated randomly by movement of a structural unit in the unit cell, and each structure is then assessed by a comparison between the calculated and measured diffraction patterns. In this case, the complexity of a direct-space search procedure depends strongly on the number of degrees of freedom in the optimization rather than on the number of atoms in the asymmetric unit. For inclusion compounds encaging a stoichiometric number of guest molecules, the main advantage of the direct-space technique is the possibility of actually refining the dynamical disorder of guest molecules in the cages.

In this article, the ab initio crystal structural determination of gas hydrate structures I, II, and H by the direct-space and the Rietveld refinement techniques using powder X-ray diffraction (PXRD) data is reported. Again, many crystal structures of gas hydrates have been solved by assuming the atomic positions, including disorder, for structural refinement by means of powder diffraction. Such assumptions often are acceptable for rare gas molecules, such as Xe, Kr, and Ar, and spherical or small symmetrical molecules such as CH_4. However, it is unclear that this assumption is acceptable for nonspherical molecules such as hydrogen and larger guest molecules such as propane and other hydrocarbons, especially for guests in nonspherical cavities. It has also been reported from single

(15) Ripmeester, J. A.; Ratcliffe, C. I.; Udachin, K. A. Clathrate Hydrates. In *Encyclopedia of Supramolecular Chemistry*; Atwood, J. A., Steed, J., Eds.; Marcel Dekker, Inc.: New York, 2004; pp 274−280.
(16) Müller, H. R.; Stackelberg, M. V. *Naturwissenschaften* **1952**, *39*, 20.
(17) Stackelberg, M. V.; Müller, H. R. *Naturwissenschaften* **1951**, *38*, 456.
(18) Ripmeester, J. A.; Tse, J. S.; Ratcliffe, C. I.; Powell, B. M. *Nature* **1987**, *325*, 135−136.
(19) McMullan, R. K.; Jeffrey, G. A. *J. Chem. Phys.* **1965**, *42*, 2725.
(20) Mak, T. C. W.; McMullan, R. K. *J. Chem. Phys.* **1965**, *42*, 2732.
(21) Udachin, K. A.; Ratcliffe, C. I.; Enright, G. D.; Ripmeester, J. A. *Supramol. Chem.* **1997**, *8*, 173−176.
(22) Udachin, K. A.; Enright, G. D.; Ratcliffe, C. I.; Ripmeester, J. A. *J. Am. Chem. Soc.* **1997**, *119*, 11481−11486.
(23) Udachin, K. A.; Ripmeester, J. A. *Nature* **1999**, *397*, 420−423.
(24) Udachin, K. A.; Ratcliffe, C. I.; Ripmeester, J. A. *Angew. Chem., Int. Ed.* **2001**, *40*, 1303−1305.
(25) Kirchner, M. T.; Boese, R.; Billups, W. E.; Norman, L. R. *J. Am. Chem. Soc.* **2004**, *126*, 9407−9412.

(26) Ikeda, T.; Mae, S.; Yamamuro, O.; Matsuo, T.; Ikeda, S.; Ibberson, R. M. *J. Phys. Chem. A* **2000**, *104*, 10623−10630.
(27) Henning, R. W.; Schultz, A. J.; Thieu, V.; Halpern, Y. *J. Phys. Chem. A* **2000**, *104*, 5066−5071.
(28) Gutt, C.; Asmussen, B.; Press, W.; Johnson, M. R.; Handa, Y. P.; Tse, J. S. *J. Chem. Phys.* **2000**, *113*, 4713−4721.
(29) Chazallon, B.; Kuhs, W. F. *J. Chem. Phys.* **2002**, *117*, 308−320.
(30) Rawn, C. J.; Rondinone, A. J.; Chakoumakos, B. C.; Circone, S.; Stern, L. A.; Kirby, S. H.; Ishii, Y. *Can. J. Phys.* **2003**, *81*, 431−438.
(31) Jones, C. Y.; Marshall, S. L.; Chakoumakos, B. C.; Rawn, C. J.; Ishii, Y. *J. Phys. Chem. B* **2003**, *107*, 6026−6031.
(32) Rondinone, A. J.; Chakoumakos, B. C.; Rawn, C. J.; Ishii, Y. *J. Phys. Chem. B* **2003**, *107*, 6046−6050.
(33) Lokshin, K. A.; Zhao, Y.; He, D.; Mao, W. L.; Mao, H. K.; Hemley, R. J.; Lobanov, M. V.; Greenblatt, M. *Phys. Rev. Lett.* **2004**, *93*, 125503.
(34) Hester, K. C.; Strobel, T. A.; Sloan, E. D.; Koh, C. A.; Huq, A.; Schultz, A. J. *J. Phys. Chem. B* **2006**, *110*, 14024−14027.
(35) Hoshikawa, A.; Igawa, N.; Ymaguchi, H.; Ishii, Y. *J. Chem. Phys.* **2006**, *125*, 34505.
(36) Strobel, T. A.; Hester, K. C.; Sloan, E. D.; Koh, C. A. *J. Am. Chem. Soc.* **2007**, *129*, 9544−9545.
(37) Rietveld, H. M. *J. Appl. Crystallogr.* **1969**, *2*, 65−71.
(38) Cheetham, A. K. In *The Rietveld Method*; Young, R. A., Ed.; Oxford University Press: New York, 1993; pp 276−292.
(39) David, W. I. F.; Shankland, K.; McCusker, L. B.; Baerlocher, Ch. *Structure Determination from Powder Diffraction Data*; Oxford University Press: New York, 2002.
(40) David, W. I. F.; Shankland, K. *Acta Crystallogr.* **2008**, *A64*, 52−64.
(41) Harris, K. D. M.; Cheung, E. Y. *Chem. Soc. Rev.* **2004**, *33*, 526−538.

crystal X-ray diffraction and theoretical calculations[42−44] that larger guest molecules are not located at the center of the cages in the hydrates. The hydrate structures solved by this new approach are in good agreement with the previously determined gas hydrate structures from single crystal X-ray diffraction without any constraints on the positions of the guest molecules. Accordingly, we conclude that the methodology reported here is useful to further understand the cage occupancies and dynamics of guest molecules in inclusion compounds encaging a stoichiometric number of guest molecules in addition to the gas hydrates studied here. Moreover, the cage occupancies and guest disorder of previously unknown structures of the double hydrates of neohexane (NH) and *tert*-butyl methyl ether (TBME) with CH_4 in structure H hydrate were also determined and discussed, comparing our results with those from solid-state ^{13}C NMR and molecular dynamics (MD) simulations.

Experimental Section

Gas hydrate samples were synthesized from fine hexagonal ice (Ih) crystals by grinding the ice with stainless steel rods in a continuous rotating cylindrically shaped high-pressure cell. The high-pressure cell was loaded with hydrate-forming gas and kept at temperatures between 263 K and just below the melting point of ice Ih (273 K).[45] This procedure was continued for at least 3 days to achieve high hydrate conversions from ice. The crystallite size of each powder sample synthesized was determined by measuring their Debye−Scherrer rings as it is important to eliminate preferred orientation effects of the crystallites when recording PXRD data. The Debye−Scherrer rings were collected with a CCD diffractometer (BRUKER axs model SMART CCD) using Mo Kα radiation ($\lambda = 0.7107$ Å).

PXRD measurements were performed on a laboratory X-ray diffractmeter (40 kV, 40 mA; BRUKER model D8 Advance equipped with a solid state detector model LynxEye) in θ/θ step scan mode using Cu Kα radiation ($\lambda = 1.5406$ Å) with a step width of 0.01966° in the 2θ range of 5.0−90.0°. Fine powder hydrate samples were mounted on a PXRD sample holder made of Cu 2.5 mm in thickness under a dry N_2 gas atmosphere, evaporated from liquid N_2, and at a temperature comparable to liquid N_2 (∼100 K). Each PXRD measurement was taken at 163 K under a dry N_2 gas atmosphere using a low-temperature chamber for PXRD measurements (Anton Paar model TTK 450).

Relative cages occupancies in hydrates were obtained by solid-state ^{13}C NMR using a Bruker DSX-400 instrument (magnetic field of 9.4 T). All experiments were performed with a Bruker BL7 magic angle spinning (MAS) triple resonance probe. The spinning speed and the temperature inside the probe were controlled using standard Bruker equipment. Hydrate samples were packed in 7 mm zirconia rotors in liquid nitrogen, and the measurements were performed at 173 K. All ^{13}C NMR spectra were recorded at ∼2.5 kHz spinning rate. Single pulse excitation (90° pulse of 5 μs) with high power composite pulse proton decoupling were employed. The pulse repetition delay in these quantitative experiments was set at 300 s, which was found to be sufficient for a complete relaxation of all carbon resonances for the hydrates studied. The cross-polarization technique was also employed to distinguish the signals from the solid phase and nonhydrated liquid hydrocarbons. The high frequency signal of adamantane was used as a secondary chemical shift reference set to 38.56 ppm at 298 K.

Structural Analysis

Structure solution calculations of gas hydrates involving guest molecules were initiated by a global optimization of experimental PXRD profiles using a parallel tempering approach implemented in the direct-space technique program FOX.[46,47] Here, the space group was fixed according to those previously reported for structures I, II, and H, respectively. Also, water molecules composing the host cages were fixed at the same positions in a unit cell of each gas hydrate as previously reported. A large number of trial structures were calculated by random rotation and translation of guest molecules, taking into account their van der Waals diameter and cage occupancy changes. Here, it should be noted that almost the same optimized distributions of the guest molecules were obtained by the direct-space technique independent of initial positions of the guest molecules in the host cages.

Using the optimized model from the direct-space technique, refinement of the crystal structures was performed by the Rietveld method using the RIETAN-2000 program,[48] and the solved structures were visualized by the VESTA program.[49] Because guest molecules in the hydrate host cages may not be distorted by the van der Waals interactions between guest and host water molecules (unless there are additional low energy conformations), rigid-body constraints were used to solve the disorder of guest molecules. Although the scattering amplitude of hydrogen atom is quite small, their contribution to diffraction intensities should not be neglected. Here, virtual chemical species, *Wa* and *M*, whose atomic scattering factors are equal to the sum of those for H_2O and CH_4, $-CH_3$, or $-CH_2$, were used instead of refining hydrogen positions. Cage occupancies were used as free parameters in the refinement. After each refinement, length between host water molecules and guest molecules were checked according to their van der Waals radius. The error in the cage occupancy fraction was estimated by varying the displacement parameters between reasonable limits as these and the occupancy factors were coupled. During the Rietveld refinement process, each atomic position of oxygen in water molecules, represented by the virtual chemical species *Wa,* was also refined.

Results and Discussion

As expected, CO_2 and C_2H_6 hydrates were structure I, and C_3H_8 hydrate was structure II. MCH + CH_4, NH + CH_4, and TBME + CH_4 binary hydrates were structure H. The initial crystallographic model for the host structures composed of water molecules was introduced from the previously reported models of X-ray diffraction data of CH_4 hydrate[28] for structure I hydrate, C_3H_8 hydrate[19] for structure II hydrate, and MCH + CH_4 hydrate[43] for structure H hydrate. Accordingly, all PXRD data was analyzed for the entire pattern, fitting by means of the direct-space technique followed by Rietveld refinement. Because the measured diffraction patterns revealed that the hydrate samples were mixtures of gas hydrate and a small amount of unreacted ice Ih of space group $P6_3/mmc$, multiphase refinement was performed. Crystal data refined in this study are summarized in Table 1.

Structure I CO_2 Hydrate. Figure 2a shows the CO_2 molecules with full symmetry in small and large cages in cubic structure I analyzed by Rietveld refinement (Table S1 and Figure S1 in Supporting Information). In the large cage, the guests lie near to the equatorial plane of the cage, and the refinement forces the long axis of the guest to lie in the plane. The center of the CO_2 molecule lies 0.5755(2) Å out off the center of the equatorial plane of the cage. The best model derived using this

(42) Udachin, K. A.; Ratcliffe, C. I.; Ripmeester, J. A. *J. Phys. Chem. B* **2001**, *105*, 4200–4204.
(43) Udachin, K. A.; Ratcliffe, C. I.; Ripmeester, J. A. *J. Supramol. Chem.* **2002**, *2*, 405–408.
(44) Fujii, K.; Arata, Y.; Tanaka, H.; Nakahara, M. *J. Phys. Chem. A* **1998**, *102*, 2635–2640.
(45) Handa, Y. P. *J. Chem. Thermodyn.* **1986**, *18*, 891–902.

(46) Favre-Nicolin, F.; Cerny, R. *J. Appl. Crystallogr.* **2002**, *35*, 734–743.
(47) Cerny, R.; Favre-Nicolin, F. *Z. Kristallogr.* **2007**, *222*, 105–113.
(48) Izumi, F.; Ikeda, T. *Mater. Sci. Forum* **2000**, *321−324*, 198–204.
(49) Monma, K.; Izumi, F. *J. Appl. Crystallogr.* **2008**, *41*, 653–658.

Table 1. Crystallographic Information and Refinement Information[a]

	guest(s)					
	CO_2	C_2H_6	C_3H_8	MCH + CH_4	NH + CH_4	TBME + CH_4
crystal system	cubic	cubic	cubic	hexagonal	hexagonal	hexagonal
space group	$Pm3n$	$Pm3n$	$Fd3n$	$P6/mmm$	$P6/mmm$	$P6/mmm$
unit cell dimension, Å						
a	11.879(6)	12.009(3)	17.174(4)	12.203(7)	12.2389(4)	12.2375(6)
c				10.056(4)	10.0547(5)	10.0282(6)
unit cell volume, Å³	1676(1)	1732.0(7)	5066(1)	1297(1)	1304.3(1)	1300.6(1)
cage occupancies, %						
small	69	12	0	100	79	77
medium				91	88	85
large	99	98	92	100	98	100
empirical formula	$(CO_2)_{7.3}(H_2O)_{46}$	$(C_2H_6)_{6.1}(H_2O)_{46}$	$(C_3H_8)_{7.4}(H_2O)_{136}$	$C_6H_{14}(CH_4)_{4.8}(H_2O)_{34}$	$C_6H_{14}(CH_4)_{4.2}(H_2O)_{34}$	$C_5H_{12}O(CH_4)_{4.1}(H_2O)_{34}$
D_{cal}, g cm⁻³	1.139	0.970	0.910	1.009	0.972	0.969
Rwp, %	10.1	10.6	11.2	11.0	11.5	11.4
goodness of fit, χ^2	5.3	5.4	5.7	5.3	5.6	5.6

[a] The errors of the cage occupancies are ±2%.
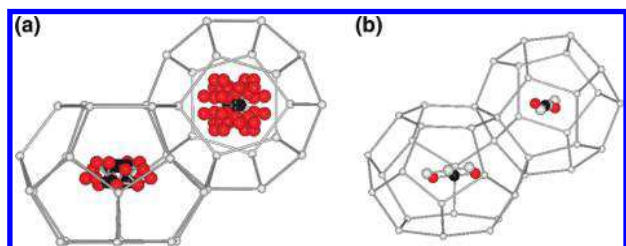

Figure 2. (a) CO_2 molecules (carbon atom, black; oxygen atom, red) in structure I large ($5^{12}6^2$) and small (5^{12}) cage with full symmetry shown. (b) CO_2 molecules in CO_2 hydrate found in this study and by the single crystal X-ray diffraction (gray) reported by Udachin et al.[42] for comparison. On the left is the structure I large cage and on the right is the small (5^{12}) cage.

procedure shows that the CO_2 guest in each large cage has its long axis at an angle of 8° to the equatorial plane. The disordered guest in the small pentagonal dodecahedral cage is best modeled by allowing the carbon in the CO_2 molecule to be located almost at the center of the cage. The refined model showed that CO_2 occupied 99% of the large cages and 69% of the small cages in this study, whereas these values were previously reported[42] to be 100% and 71% from single crystal analysis. Figure 2b shows the comparison of CO_2 positions in small and large cages refined by PXRD with those from single crystal analysis. Consequently, the cage occupancies and the disordered model of CO_2 in large and small cages are quite consistent for previous single crystal X-ray results carried out at 173 K. The result is also consistent with results by ¹³C NMR and MD simulations.[50]

On the other hand, an earlier powder neutron diffraction study[26] suggested that CO_2 molecules make an angle of 31° with the equatorial plane in the temperature range between 5 and 205 K by assuming the carbon atom of the disordered CO_2 molecules to be at the center of the cage. In this study, a CO_2 occupancy of 100% of the large cage and 99% of the small cage were reported.[26] Another earlier powder neutron diffraction study suggested that the CO_2 guest in each large cage lies in the equatorial plane of the cage at 14 K by assuming the carbon atom of the disordered CO_2 molecule to be at the center of the cages, and a CO_2 occupancy of >95% of the large cage and 60−80% of the small cage were reported.[27] The discrepancy between the results on the disordered model for CO_2 may well be caused by the assumption of the position of the carbon atom
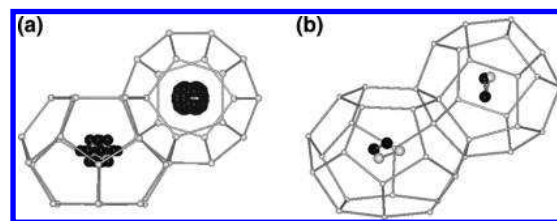

Figure 3. (a) C_2H_6 molecules in the structure I large ($5^{12}6^2$) and small (5^{12}) cages shown with full symmetry. Solid spheres express the virtual chemical species, -CH_3, shown *M*. (b) C_2H_6 molecules in C_2H_6 hydrate found in this study (black) and by the single crystal X-ray diffraction (gray) reported by Udachin et al.[43] for comparison.

as the displacement parameter, which represents atomic motions and a possible static displacive disorder, and the cage occupancies are coupled.

Structure I C_2H_6 Hydrate. Figure 3a shows the C_2H_6 molecules with full symmetry in small and large cages in cubic structure I analyzed by Rietveld refinement (Table S2 and Figure S2 in Supporting Information). In the large cages, the center of the C_2H_6 molecule lies 0.5530(1) Å out off the center of the equatorial plane of the cage, and makes an angle of 23° with the equatorial plane. Figure 3b shows the comparison of C_2H_6 positions refined by PXRD with single crystal analysis. The refined model showed that C_2H_6 occupied 98% of the large cages and 12% of the small cages in this study, whereas it was found to be 100% of the large cages and 5.8% of the small cages by single crystal analysis in the earlier study.[43] Comparison with NMR data obtained earlier[51] and this study showed that the low occupancy of the small cage was not picked up in the ²H NMR experiment. However, the out-of-plane angle of 23° obtained from the structural model compares well with the angle worked out from one of the ²H NMR model:[51] a value of 25.2° was found by assuming that molecule rotates about the cage symmetry axis at a constant angle to the equatorial plane.

Structure II C_3H_8 Hydrate. Figure 4a shows the C_3H_8 molecules with full symmetry in the large cage of cubic structure II analyzed by Rietveld refinement (Table S3 and Figure S3 in Supporting Information). The center of the C_3H_8 molecule in the large cage lies 0.8092(1) Å out off the center of the equatorial plane of the cage. Figure 4b shows a comparison of the C_3H_8 position refined by PXRD with single crystal analysis. Even if we use single crystal X-ray diffraction data, it is still

(50) Alavi, S.; Dornan, P.; Woo, T. K. *ChemPhysChem.* **2008**, *9*, 911–919.

(51) Davidson, D. W.; Ratcliffe, C. I.; Ripmeester, J. A. *J. Inclusion Phenom.* **1984**, *2*, 239–247.
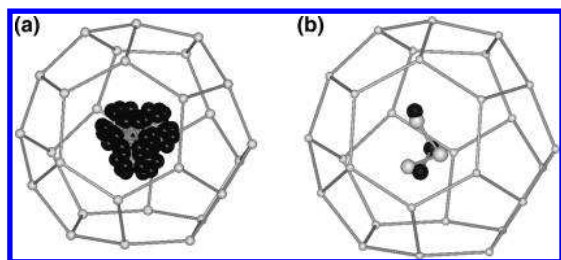
Figure 4. (a) C_3H_8 molecules in structure II large ($5^{12}6^4$) with full symmetry shown. Solid spheres express the virtual chemical specie, $-CH_2$ and $-CH_3$, shown *M*. (b) C_3H_8 molecules in C_3H_8 hydrate found in this study (black) and by the single crystal X-ray diffraction (gray) reported by Udachin et al.[52] for comparison. Only the large ($5^{12}6^4$) cage of structure II is shown.
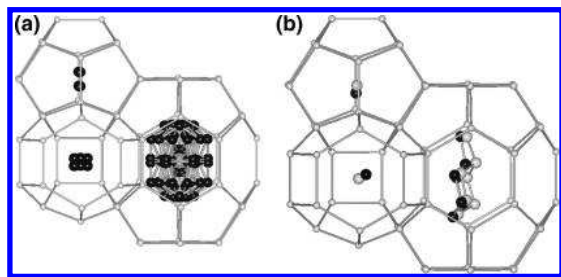

Figure 5. (a) MCH and CH_4 molecules in structure H large ($5^{12}6^8$), medium ($4^35^66^3$), and small (5^{12}) cage with full symmetry shown. Solid spheres express the virtual chemical species, $-CH_2$, $-CH_3$, and CH_4, shown *M*. (b) MCH and CH_4 molecules in MCH + CH_4 hydrate found in this study (black) and by the single crystal X-ray diffraction (gray) reported by Udachin et al.[43] for comparison. At the left top is the small (5^{12}) cage, on the left bottom is the medium ($4^35^66^3$) cage, and on the right is the large ($5^{12}6^8$) cage of structure H.

not trivial to refine atomic positions of guest molecules as reported previously.[52] Therefore, the consistency of the positions of C_3H_8 molecule in the large cages between the result in this study and the result of the earlier study by means of single crystal X-ray diffraction suggest that it is reasonable to introduce rigid-body constraints in the PXRD refinements. The refined model showed that C_3H_8 occupied 92% of the large cages and 0% of the small cages in this study, whereas it was found 100% of the large cages and 0% of the small cages were occupied in the single crystal analysis.[52]

Structure H MCH + CH_4 Hydrate. Figure 5a shows the MCH molecules in the large cage and the CH_4 molecules in small and medium cages in hexagonal structure H analyzed by Rietveld refinement (Table S4 and Figure S4 in Supporting Information). The refined PXRD results showed that CH_4 occupied 100% of the small cages and 91% of the medium cages and MCH occupied 100% of the large cages in this study, whereas the single crystal analysis found that CH_4 occupied 82% of the small cages and 81% of the medium cages and MCH occupied 100% of the large cages.[43] The cage occupancies of MCH + CH_4 hydrate synthesized in the same batch as the sample for the PXRD measurements are in good agreement with the ^{13}C NMR data: CH_4 occupied 90% of the small cages, and 99% of the medium cages and MCH occupied 100% of the large cages. Figure 5b shows a comparison of MCH and CH_4 positions refined by PXRD with single crystal analysis. The disordered guest molecule positions found in this study are in
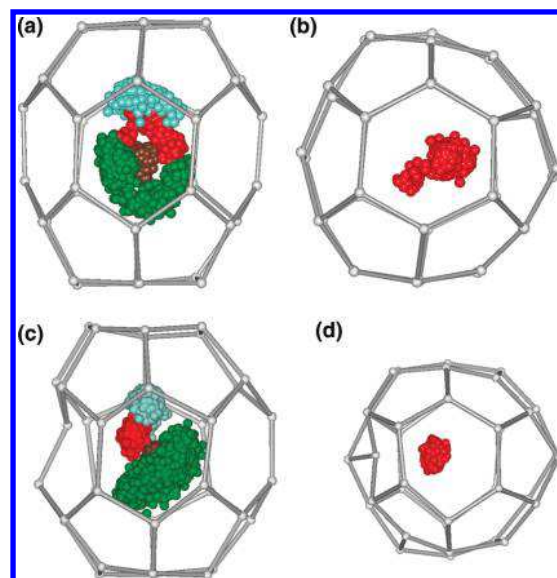

Figure 6. (a) View of NH molecules in the structure H large ($5^{12}6^8$) cage. Each symbolic number of the virtual chemical species corresponds to those shown in Table S5 in Supporting Information. (b) NH molecule in structure H large ($5^{12}6^8$) cage with full symmetry shown. Here, atomic bonding is not shown in order to see each atom easily.

good agreement with those found by the single crystal X-ray diffraction technique in the earlier study.[43]

Overall, it is shown that the positions of dynamically disordered guest molecules determined in this study are consistent with these refined by the single crystal diffraction technique for different samples, as noted above. The absolute cage occupancies determined in this study are also consistent with those refined by the single crystal diffraction technique. Therefore, we conclude that the analytical methodology reported in this study is suitable to solve guest disorder and cage occupancies of gas hydrates using PXRD data. For more detailed comparisons, however, small differences in cage occupancies are expected due to the different gas hydrate formation conditions as earlier macroscopic measurements show small changes of hydration numbers due to changes in formation pressures.[53,54] In this study, the hydrates were formed at higher pressures than that required for equilibrium conditions, taking about three days, whereas the hydrates for the single crystal study was synthesized closer to equilibrium, taking at least several months. According to the earlier studies,[53,54] the changes of cage occupancy for a variety of gas hydrates are estimated to be roughly less than 10% for small cages by assuming full cage occupancy for the large cage. For further discussions on absolute values of cage occupancy, comparison of some identical gas hydrate formed under different conditions will work.

Structure H NH + CH_4 Hydrate and TBME + CH_4 Hydrate. Structural analysis of the previously unknown structures H NH + CH_4 hydrate and TBME + CH_4 hydrate were also performed in this way. The configuration and van der Waals diameter of NH and TBME molecule is almost the same. Then the comparison of their detailed structure is good example for understanding guest−host interactions of clathrate hydrate.

Figure 6a shows the NH molecule in the large cage in hexagonal structure H analyzed by Rietveld refinement (Table S5 and Figure S5 in Supporting Information). The NH molecules

(52) Udachin, K. A.; Lu, H.; Enright, G. D.; Ratcliffe, C. I.; Ripmeester, J. A.; Chapman, N. R.; Riedel, M.; Spence, G. *Angew. Chem., Int. Ed.* **2007**, *46*, 8220–8222.

(53) Candy, G. H. *J. Phys. Chem.* **1981**, *85*, 3225–3230.
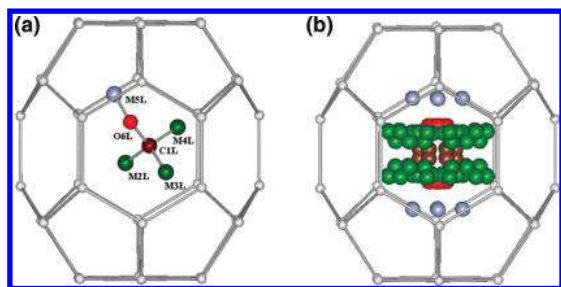(54) Candy, G. H. *J. Phys. Chem.* **1983**, *87*, 4437–4441.

Figure 7. (a) View of TBME molecule in the structure H large $(5^{12}6^8)$ cage. Each symbolic number of the virtual chemical species corresponds to those shown in Table S6 in Supporting Information. (b) TBME molecule in structure H large $(5^{12}6^8)$ cage shown with full symmetry. Here, atomic bonding is not shown in order to see each atom easily.

with full symmetry in the large cage in structure H are shown in Figure 6b. The refined model showed that CH_4 occupied 79% of the small cages and 88% of the medium cages and NH occupied 100% of the large cages in this study. The cage occupancies of NH + CH_4 hydrate synthesized in the same batch as the sample for the PXRD suggest good agreement between PXRD result and ^{13}C NMR result: CH_4 occupied 86% of the small cage and 87% of the medium cage and NH occupied 100% of the large cage by ^{13}C NMR. Figure 7a shows the TBME molecule in the large cage in hexagonal structure H analyzed by Rietveld refinement (Table S6 and Figure S6 in Supporting Information). The refined model showed that CH_4 occupied 77% of the small cages and 85% of the medium cages and TBME occupied 98% of the large cages in this study. The cage occupancies of TBME + CH_4 hydrate synthesized in the same batch as the sample for the PXRD show good agreement between PXRD and ^{13}C NMR results: CH_4 occupied 75% of the small cage and 89% of the medium cage and TBME occupied 100% of the large cage by ^{13}C NMR. From the analytical results in this study, it is shown that the NH molecule carbon atoms, which are noted as *C1L* in Figure 6a, point toward the six-ring faces of the large cage of structure H hydrate facing the *c*-axis with 18° deviation (see Figure 6b). On the other hand, the TBME molecule oxygen atoms, noted as *O6L* in Figure 7a, point toward the six-ring faces of the large cage of structure H hydrate facing the *c*-axis with 19° deviation (see Figure 7b). It is shown that the guest dynamical disorder of NH and TBME is different while the configurations of the guest molecules is almost the same for NH and TBME (see Figures 6 and 7). It suggests that the presence of an oxygen atom in the TBME molecule may affect the dynamics of the guest molecule in the cage of structure H hydrate.

Figure 8 shows ^{13}C CP MAS NMR spectra of NH + CH_4 and TBME + CH_4 hydrate as a function of temperature. By reducing temperature, changes in the width of the signals were observed especially for the signal in NH at around 29 ppm and signals in TBME at around 27 and 48 ppm at 153 K. Since the spin−lattice relaxation times for all carbon atoms in enclathrated molecules change very little over the range of temperatures studied,[55] the observed increase in the line widths can be attributed to a distribution of the chemical shifts for the guest molecules in disordered positions in the hydrate cages. It is also reported that the formation of long-lived hydrogen bonding between TBME guest molecule and host water, leading by the formation of a Bjerrum L-defect in the water lattice, restrict
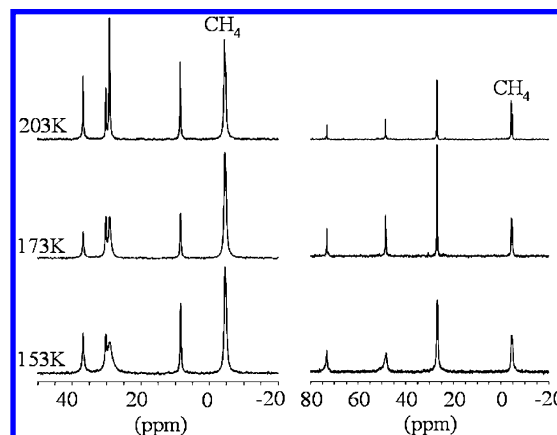
(55) Susilo, R.; Alavi, S.; Moudrakovski, I. L.; Englezos, P.; Ripmeester, J. A. *ChemPhysChem.* **2009**, *10*, 824–829.

Figure 8. ^{13}C CP MAS NMR spectra of structure H hydrate as a function of temperature. (Left) NH + CH_4 hydrate. (Right) TBME + CH_4 hydrate.
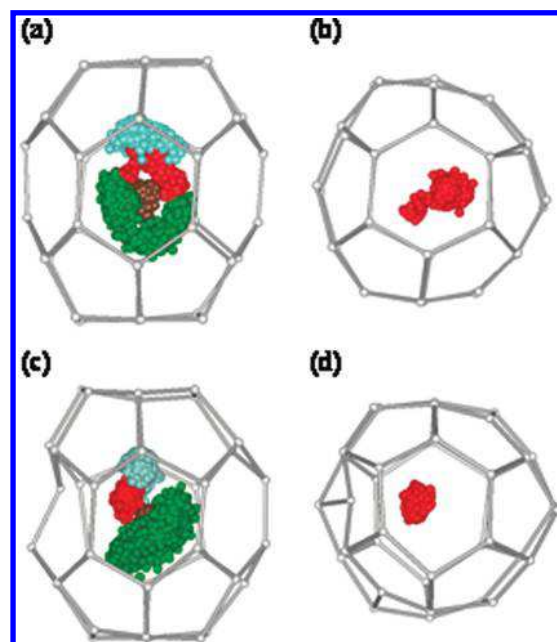

Figure 9. Snapshots of the orientation of guest molecules in the structure H large $(5^{12}6^8)$ cage superimposed over 200 ps at 150 K by MD simulations. Each color of the guest molecules corresponds to those shown in Figures 6 and 7. (a) View of NH molecules. (b) View of only C2L carbon atom in the NH molecule from the direction of the *c*-axis. (c) View of TBME molecules. (d) View of only oxygen atoms in TBME atom from the direction of the *c*-axis. There is one water of the cage pointed toward the TMBE oxygen.

rattling and rotational motions of TBME compared to NH by using MD simulation.[55] As is shown in Figure 9, snapshots of orientation of TBME and NH molecules in the structure H large cage superimposed over 200 ps at 150 K by MD simulations are similar to the disordered models refined in this study, even though the simulation time does not allow one to observe fully disordered distribution of the guest molecules.

In the case of the crystal structure of TBME + CH_4 hydrate refined in this study, the shortest distance between the oxygen atom on the TBME molecule and the oxygen atom on the water molecule in the large host cage is 4.329(4) Å. It shows that, on average, there is no strong guest−host interaction between these two atoms such as hydrogen bonding. Bond lengths in the pentagonal and hexagonal planes forming the large cages of structure H hydrates presented in Figure 10 are summarized in
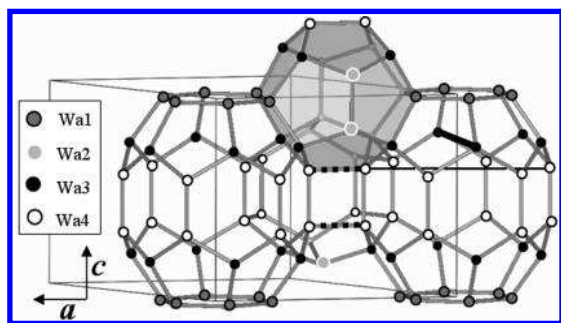
Figure 10. Detailed polyhedral large ($5^{12}6^8$), medium ($4^3 5^6 6^3$), and small (5^{12}) cage in structure H hydrate along the *a*-axis. Here, the small cage is hatched. The bold and fine solid lines show the shortest and longest diameter of the equatorial plane of the large cage, respectively. Each symbolic number of the virtual chemical species corresponds to those shown in Tables S4–S6 in Supporting Information.

Table 2. Bond Lengths in the Pentagonal and Hexagonal Planes Forming the Large Cages of Structure H Hydrates

guests	Wa1–Wa1	distance, Å Wa3–Wa4	distance, Å Wa4–Wa4	distance, Å Wa1–Wa3
MCH + CH$_4$	2.772(3)	2.770(3)	2.753(6)	2.788(3)
NH + CH$_4$	2.776(3)	2.756(3)	2.793(5)	2.795(3)
TBME + CH$_4$	2.766(3)	2.758(3)	2.768(6)	2.783(4)

Table 3. Structure H Hydrate Cage Dimensions for the Three Hydrates Refined in This Study[a]

guests	distance between large cages, Å Wa4–Wa4	shortest diameter of large cage, Å Wa3–Wa3	longest diameter of large cage, Å Wa4–Wa4
MCH + CH$_4$	2.7423(9)	8.843(4)	9.461(3)
NH + CH$_4$	2.7826(3)	8.854(2)	9.4563(4)
TBME + CH$_4$	2.8511(4)	8.865(2)	9.3864(5)

[a] The shortest and longest diameters are represented by solid lines in Figure 10.

Table 2, which shows that these bond lengths are 2.77(3) Å in the three hydrates. However, the Wa4–Wa4 bond length represented by a dotted line in Figure 10 for TBME + CH$_4$ hydrate of 2.852(5) Å is apparently longer than other bond lengths as summarized in Table 3. It also shows that the largest diameter of the equatorial plane of the large cage shown in Figure 10 in TBME + CH$_4$ hydrate is shorter than those in NH + CH$_4$ and MCH + CH$_4$ hydrates, whereas the shortest diameter of the equatorial plane of the large cage is almost the same in the three hydrates. Because the unit cell *a*-axes are almost the same for the case of NH + CH$_4$ hydrate and TBME + CH$_4$ hydrate (see Table 1), host cages of structure H hydrate are slightly distorted depending on the type of guest molecule. It is also shown that the displacement parameters, *B*, of the host water molecules of TBME + CH$_4$ hydrate and NH + CH$_4$ hydrate are almost the same (see Tables S5 and S6 in Supporting Information). Therefore, the small differences in the diameter of the equatorial plane of the large cage for TBME + CH$_4$ hydrate are likely caused by the formation of the guest–host hydrogen bonding associated lattice L-defects, even though the guest–host hydrogen bonds are transient and are not stable over the lifetime of the crystal structure determination experiment by using diffraction methods.

Recently, evidence for an ordering transition in structure I trimethylene oxide (TMO) hydrate has been demonstrated by means of single crystal X-ray diffraction and ^{2}H NMR techniques, where the oxygen atom from the TMO molecules points toward the six-ring faces in the large cage of structure I hydrate

and aligns in domains at low temperatures due to the dipole moments of the guest molecules.[56] Therefore, further studies of the structures and dynamics of guest molecules may lead to additional insights into the guest dynamics and the ordering processes of gas hydrates, especially in gas hydrates where expansion or distortion of the host lattice due to the type of guest molecule has been reported previously.[57−59]

More than 2 decades ago, in contrast to prevailing opinion, it was found that structure II hydrate may also be formed by small guest molecules or atoms such as O$_2$, N$_2$, Kr, and Ar in addition to molecules larger than ~5.8 Å. Before that, it had been thought that these species formed structure I hydrate.[60−62] Naturally occurring air (N$_2$ + O$_2$) hydrate is also reported to be structure II by single crystal X-ray diffraction.[63] In the past decade, the behavior of gas hydrates containing small guest molecules have been explored under very high pressure conditions, higher than ~0.1 GPa.[64] Eventually, it was found that even the H$_2$ molecule forms structure II hydrate under very high pressure conditions.[65] On the other hand, hydrate research, including that on the semiclathrate hydrates encaging large guest molecules, is attractive as there is potential for hydrogen storage after the recent reports of H$_2$ + THF hydrate under several MPa at around the melting temperature of ice I$_h$.[66−68] The ability of the structure H hydrate to concentrate CH$_4$ or H$_2$ molecules has also attracted attention to gas storage and transportation.[69−72] The exploration of such hydrate materials necessitates dealing with larger guest molecules because THF and other molecules of similar size may fit only into the large cages, leaving the small 5^{12} cages vacant for small molecules.[73,74] Therefore, the characterization and modeling of more and more complex

(56) Udachin, K. A.; Ratcliffe, C. I.; Ripmeester, J. A. *J. Phys. Chem. B* **2007**, *111*, 11366–11372.
(57) Takeya, S.; Uchida, T.; Kamata, Y.; Nagao, J.; Kida, M.; Minami, H.; Sakagami, H.; Hachikubo, A.; Takahashi, N.; Shoji, H.; Khlystov, O.; Grachev, M.; Soloviev, V. *Angew. Chem., Int. Ed.* **2005**, *44*, 6928–6931.
(58) Takeya, S.; Hori, A.; Uchida, T.; Ohmura, R. *J. Phys. Chem. B* **2006**, *110*, 12943–12947.
(59) Udachin, K. A.; Ratcliffe, C. I.; Enright, G. D.; Ripmeester, J. A. *Angew. Chem., Int. Ed.* **2008**, *47*, 9704–9707.
(60) Davidson, D. W.; Handa, Y. P.; Ratcliffe, C. I.; Tse, J. S. *Nature* **1984**, *311*, 142–143.
(61) Davidson, D. W.; Desando, M. A.; Gough, S. R.; Handa, Y. P.; Ratcliffe, C. I.; Ripmeester, J. A.; Tse, J. S. *Nature* **1987**, *328*, 418–419.
(62) Hallbrucker, A. *Angew. Chem., Int. Ed.* **1994**, *33*, 691–693.
(63) Hondoh, T.; Anzai, H.; Goto, A.; Mae, S.; Higashi, A.; Langway, C. C. *J. Inclusion Phenom.* **1990**, *8*, 17–24.
(64) Loveday, J. S.; Nelmes, R. J. *Phys. Chem. Chem. Phys.* **2008**, *10*, 937–950.
(65) Mao, W. L.; Mao, H.; Goncharov, A. F.; Struzhkin, V. V.; Gio, Q.; Hu, J.; Shu, J.; Hemley, R. J.; Somayazulu, M.; Zhao, Y. *Science* **2002**, *297*, 2247–2249.
(66) Florusse, L. J.; Peters, C. J.; Schoonman, J.; Hester, K. C.; Koh, C. A.; Dec, S. F.; Marsh, K. N.; Sloan, E. D. *Science* **2004**, *306*, 469–471.
(67) Lee, H.; Lee, J. W.; Kim, D. Y.; Park, J.; Seo, Y. T.; Zeng, H.; Moudrakovski, I. L.; Ratcliffe, C. I.; Ripmeester, J. A. *Nature* **2005**, *434*, 743–746.
(68) Chapoy, A.; Anderson, R.; Tohidi, B. *J. Am. Chem. Soc.* **2007**, *129*, 746–747.
(69) Khokhar, A. A.; Gudmundsson, J. S.; Sloan, E. D. *Fluid Phase Equilib.* **1998**, *150−151*, 383–392.
(70) Susilo, R.; Alavi, S.; Ripmeester, J. A.; Englezos, P. *Fluid Phase Equilib.* **2008**, *263*, 6–17.
(71) Strobel, T. A.; Koh, C. A.; Sloan, E. D. *J. Phys. Chem. B* **2008**, *112*, 1885–1887.
(72) Duarte, A. R. C.; Shariati, A.; Rovetto, L. J.; Peters, C. J. *J. Phys. Chem. B* **2008**, *112*, 1888–1889.
(73) Ohmura, R.; Takeya, S.; Uchida, T.; Ikeda, I. Y.; Ebinuma, T.; Narita, H. *Fluid Phase Equilib.* **2004**, *221*, 151–156.
(74) Cha, M.; Shin, K.; Lee, H. *J. Phys. Chem. B* **2009**, *113*, 10562–10565.

hydrate inclusion compounds[75] are required not only from a scientific viewpoint but also for developing applications. Finally, it should be noted that the methodology reported here depends on the number of degrees of freedom in the optimization rather than on the number of atoms in the asymmetric unit of the crystal, which is advantageous for finding structural solutions for a variety of inclusion compounds containing a stoichiometric number of guest molecules.

Conclusions

We have demonstrated that powder X-ray diffraction analysis combined with the direct-space technique and Rietveld refinement is a powerful tool for determining gas hydrate structures and compositions. This ab initio methodology has been used successfully for hydrate crystal structure determinations from powder X-ray diffraction data and applied to solve the crystal structures of structure I, II, and H for the following guests: CO_2, C_2H_6, C_3H_8, MCH + CH_4, NH + CH_4, and TBME + CH_4. It is also possible to obtain the positions of disordered guest molecules and absolute cage occupancies of gas hydrates without the need of single crystal diffraction analysis.

As shown in this study, all guest molecules examined in this study lie off the geometrical center of the large cages. Because of strong correlations between displacement parameters and cage

occupancies, an appropriate disorder model for guest molecules needs be used, especially for larger guest molecules. The resultant cage occupancies and positions of the disordered guest molecules were in good agreement with the results reported by means of conventional experimental methods by using single crystal X-ray diffraction and ^{13}C NMR spectroscopy. Consequently, we conclude that the guest disorder model for gas hydrates as solved by the direct-space technique is satisfactory for structural analysis of nonstoichiometric guest molecules in the hydrate host cages using the Rietveld technique.

Although the examples presented here focus on the structural determination of gas hydrates, the principles of this approach are quite general, and the methodology reported in this study is also applicable to neutron powder diffraction experimental data and other guest−host materials.

(75) Jeffrey, G. A. *J. Inclusion Phenom.* **1984**, *1*, 211–222.